

Supplemental Data

Supplemental Table Legends

Supplemental Table 1. List of genes differentially regulated between LEC-*Foxc1;Foxc2*-DKO and littermate control LECs. Using the cufflinks program, unique readings were mapped on the genome and gene expression was quantified based on RPKM (reads per kilo base of coding sequence per million mapped). The fold-change values were calculated based on RPKM values between the control LECs (RPKM1) and LEC-*Foxc1;Foxc2*-DKO LECs (RPKM2) wherein a value greater than one indicated induced gene expression and a value less than one indicated repressed gene expression.

Supplemental Table 2. List of upregulated genes in *Foxc1/Foxc2*-mutant LECs. Using the cufflinks program, unique readings were mapped on the genome and gene expression was quantified based on RPKM (reads per kilo base of coding sequence per million mapped). The fold-change values were calculated based on RPKM values between the control LECs (RPKM1) and LEC-*Foxc1;Foxc2*-DKO LECs (RPKM2). The pie-charts represent predictions from gene ontology based pathway databases showing pathway analysis relating to various biological functions.

Supplemental Table 3. List of downregulated genes in *Foxc1/Foxc2*-mutant LECs. Using the cufflinks program, unique readings were mapped on the genome and gene expression was quantified based on RPKM (reads per kilo base of coding sequence per million mapped). The

fold-change values were calculated based on RPKM values between the control LECs (RPKM1) and LEC-*Foxc1*;*Foxc2*-DKO LECs (RPKM2). The pie-charts represent gene ontology-based pathway databases showing pathway analysis and predictions relating to various biological functions.

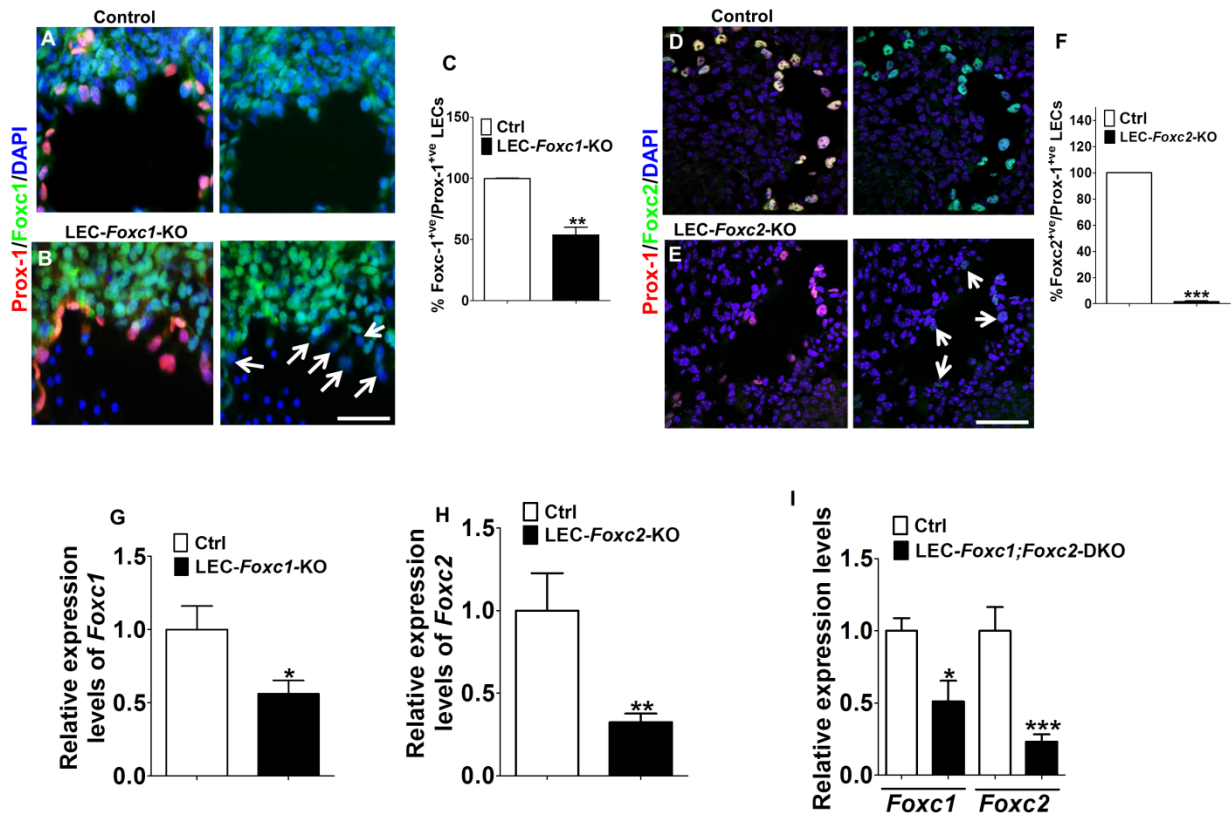
Supplemental Table 4. Primers used for qPCR analysis

| Primer | Forward | Reverse |
|---------------|-------------------------|-----------------------|
| Prox1 | TGGAGTCACCAGTACAGAAGAGC | CGCAACTTCCAGGAATCTCT |
| Foxc1 | TTCTTGCGTTCAGAGACTCG | TCTTACAGGTGAAAGGCAAGG |
| Foxc2 | AAAGCGCCCCTCTCTCAG | TCAAAGTGGAGCTGCGGATAA |
| Ppia | CAAATGCTGGACCAAACACA | TGCCATCCAGCCATTCAGTC |
| FOXC1 | TGCTTTTCAGAGACCTGCTTT | GCAAGGAAGAAGGCAAGAG |
| FOXC2 | GGGGACCTGAACCACCTC | AACATCTCCCGCACGTTG |
| GAPDH | CCAGGTGGTCTCCTCTGACTTC | GTGGTCGTTGAGGGCAAT |

Supplemental Table 5. ChIP primers

| Primer | Forward | Reverse |
|---------------|-----------------------|-----------------------|
| RASGRP3-ECR1 | AGGCTGAGATGGGAGAATCA | GCAATGTGATGGGAGTAGGG |
| RASGRP3-ECR2 | CCATTGACTTCTCCCAAGTGA | TGGGAAAGAAACAACCTGATG |
| RASA4-ECR6 | TGCTCTCGAACTCCTGACCT | TGATCTCAGTTTCCCCAAATG |
| RASA4-ECR10 | ACGCTTCTCACGGACAGAGT | ACAGTGGTTTGGATGGTTCC |
| RASA4-ECR11 | ACCCTGCCAGTATCCCCTAC | GTCTTGAGGGGGAAGAAAGG |
| RASA4-ECR17 | AGGCAGGAGAATCACTGGAA | CCTCCCCAAGTACTGGGATT |
| RASAL3-ECR2 | CACTCCCCACAACCTCCTGT | ACCAGTCGCCTTCGACTCT |
| RASAL3-ECR5 | GACTTGCTCAGGGTCACACA | CAGCCCCTGTCCTGTTTTT |
| RASAL3-ECR13 | TCCTGGAGGTAATCCTGTGC | ATCTGGTGCAACCTGACCTC |
| RASAL3-ECR17 | ATTTGGGTGCTCAGCGACT | GGGACAACGGGTCAGATTAC |

Supplemental Figure 1

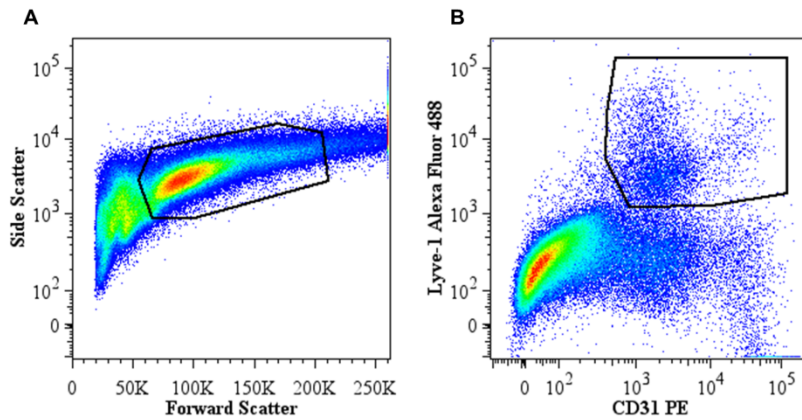


Supplemental Figure 1. Expression of *Foxc1* and *Foxc2* genes is reduced in LEC-*Foxc* mutants, confirming Cre-mediated recombination. (A-B) Prox-1/*Foxc1* immunostaining in E12.5 embryos showing a deletion of *Foxc1* gene in lymph sacs (white arrows) of LEC-*Foxc1*-KO embryos. (C) Quantification of *Foxc1*⁺/*Prox-1*⁺ LECs showing 50% deletion of *Foxc1* gene in LEC-*Foxc1*-KO embryos. n=4 (D-E) Prox-1/*Foxc2* immunostaining in E12.5 embryos showing a deletion of *Foxc2* gene in lymph sacs (white arrows) of LEC-*Foxc2*-KO embryos (F) Quantification of *Foxc2*⁺/*Prox-1*⁺ LECs showing 90% deletion of *Foxc2* gene in LEC-*Foxc2*-KO embryos. n=4. (G-I) qRT-PCR data showing decreased expression of *Foxc1* (G), *Foxc2* (H), and *Foxc1/c2* (I) in LECs isolated from E15.5 dorsal skin of LEC-*Foxc* mutants and littermate controls. The expression of *Foxc1* and *Foxc2* was normalized to internal control gene (*Ppia*). n =

5. P-values were obtained by two-tailed Student's t-test. * $p < 0.05$, ** $p < 0.01$, *** $p < 0.001$.

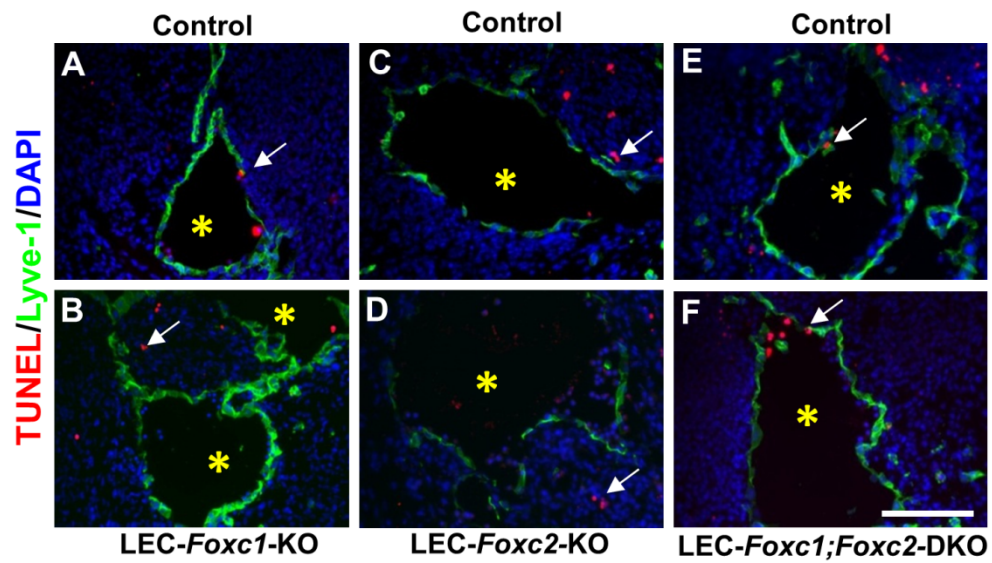
Scale bar, 50 μm .

Supplemental Figure 2



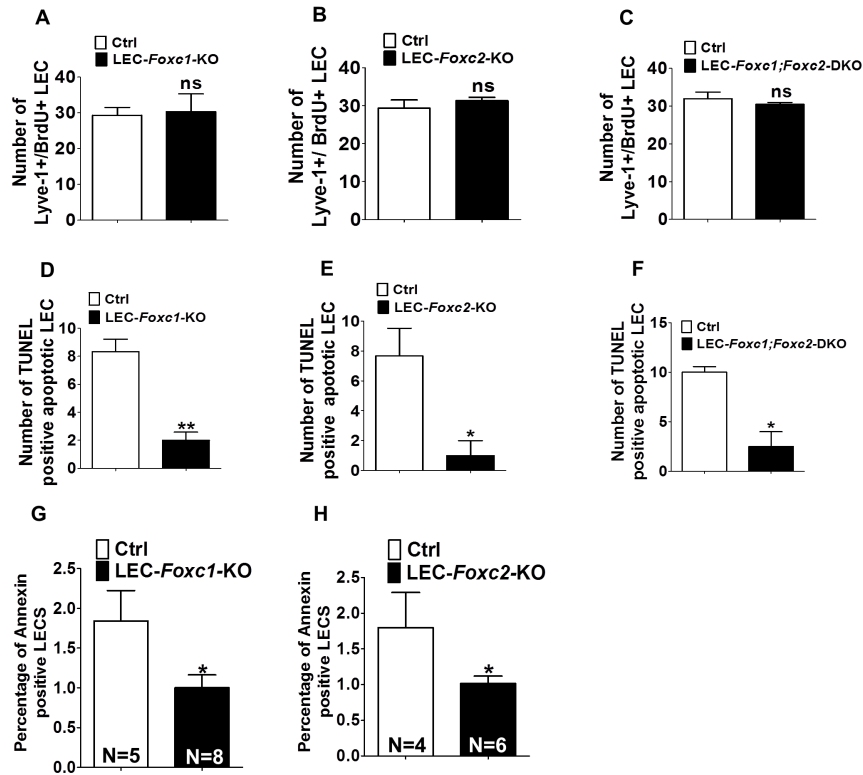
Supplemental Figure 2. Gating Scheme used for isolation of Lyve-1+/CD31+ LEC. (A, B) Dot plots showing the gating scheme used for sorting Lyve-1+/CD31+ LECs, where Gate1 (A) indicates a total live LEC population and Gate 2 (B) indicates a Lyve1+/CD31+ LEC population acquired following gating of individual CD31+ and Lyve-1+ populations, respectively.

Supplemental Figure 3



Supplemental Figure 3. Analysis of LEC survival at E12.5. (A-F) Immunostaining of E12.5 lymph sacs (asterisks) for Lyve-1 combined with TUNEL assay showing no significant difference in the number of apoptotic LECs between control and LEC-*Foxc*-KO embryos. Scale bar, 100 μ m. Arrows indicate TUNEL+ cells. Scale bar, 100 μ m.

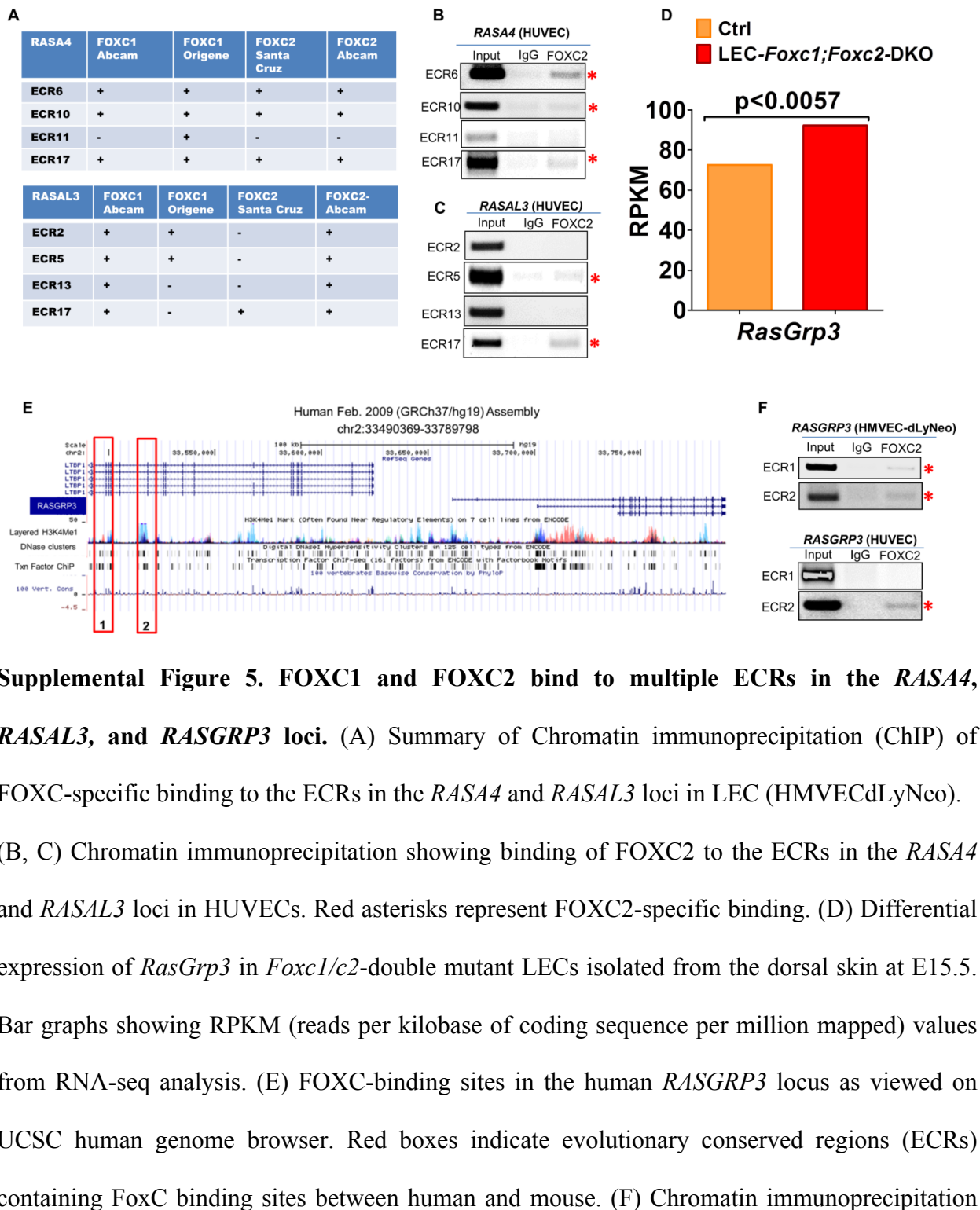
Supplemental Figure 4



Supplemental Figure 4. Analysis of LEC proliferation and survival in E15.5 dorsal skin.

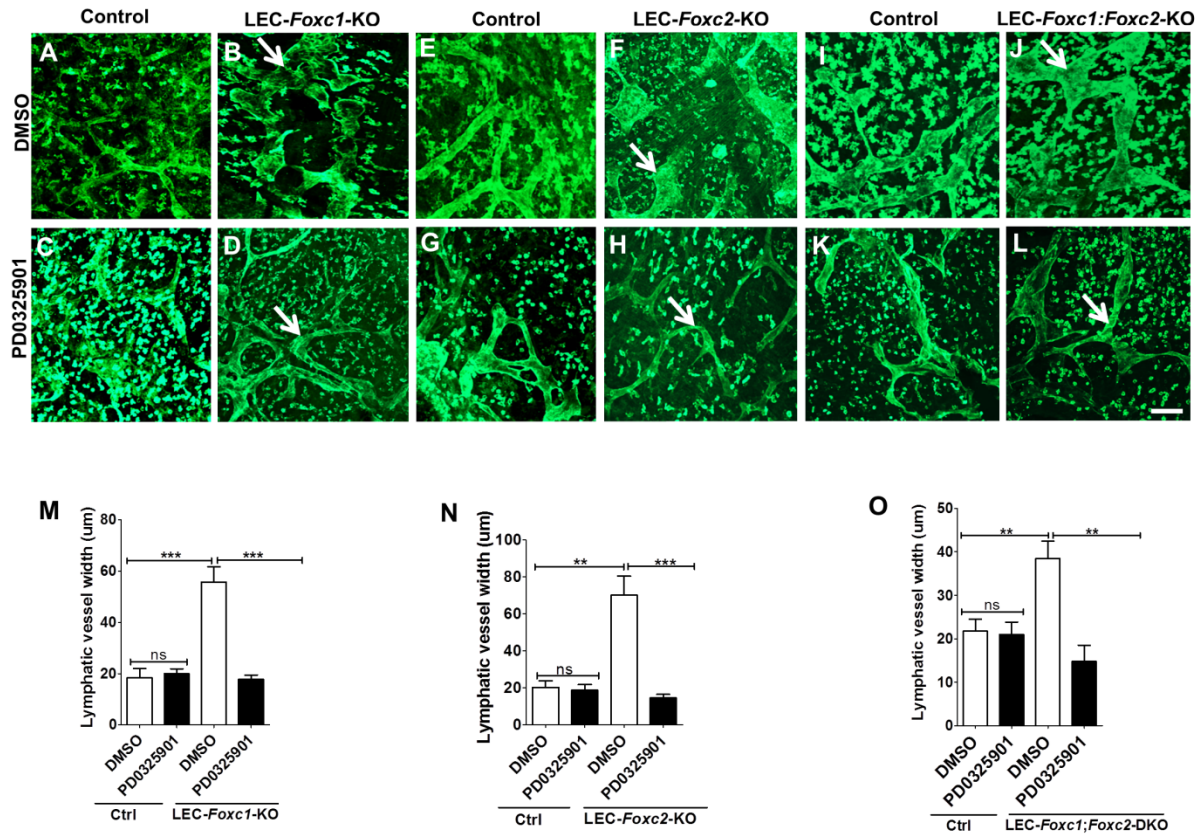
(A-C) Quantification of proliferating Lyve1+ LECs. Student's t-test. Data are presented as mean \pm SEM. n = 3. ns, non-significant. (D-F) Quantification of immunostaining for Lyve-1 with TUNEL assay. P-values were obtained by two-tailed Student's t-test. Data are presented as mean \pm SEM. n = 3. *p < 0.05, **p < 0.01. (G, H) Quantification of Annexin V+ LECs isolated from E15.5 dorsal skin. *p < 0.05.

Supplemental Figure 5



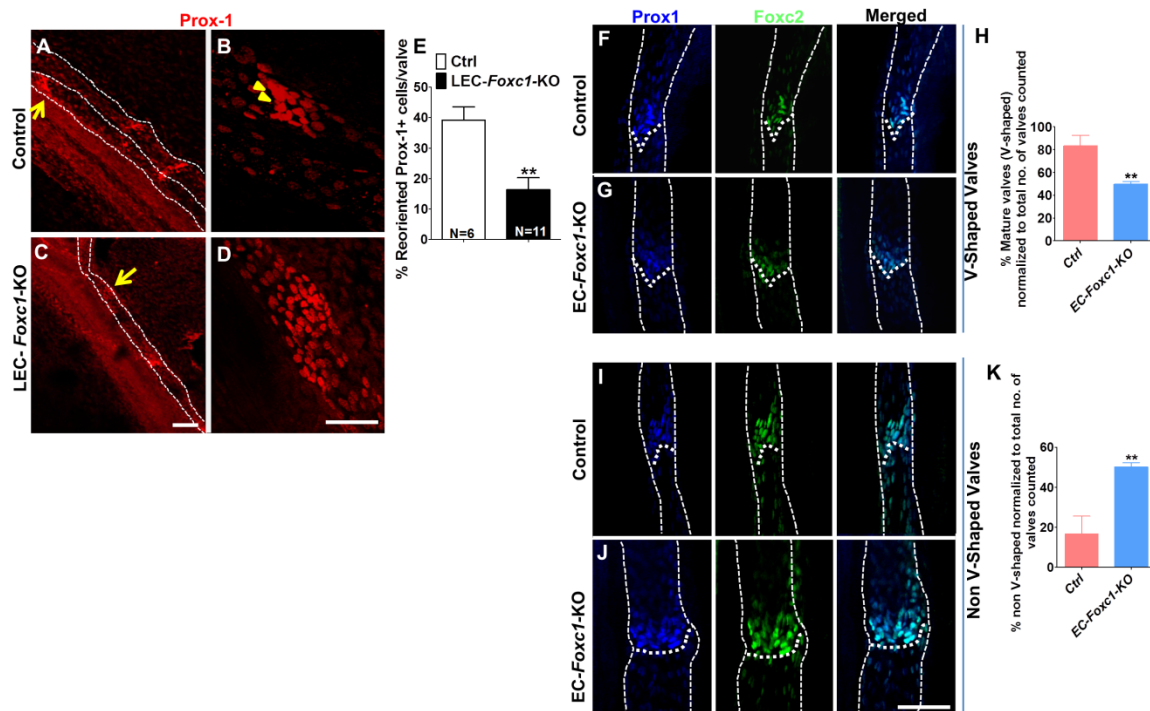
showing specific binding of FOXC2 to the *RASGRP3* ECRs in HMVEC-dLyNeo and HUVECs. Red asterisks represent FOXC2-specific binding.

Supplemental Figure 6



Supplemental Figure 6. Treatment of the MEK inhibitor PD0325901 in LEC-Foxc-KO mice rescues enlarged lymphatic vessels. Lyve-1 immunostaining of E15.5 dorsal skin (A-D, E-H, and I-L) and morphometric analysis (M, N, and O) showing the rescue of the lymphatic phenotype in all three lines of the LEC-Foxc-KO embryos by the MEK inhibitor PD0325901. n = 3. P-values were obtained by two-tailed Student's t-test. Data are presented as mean ± SEM. * p < 0.05. ** p < 0.01, *** p < 0.001. Scale bar, 50 µm.

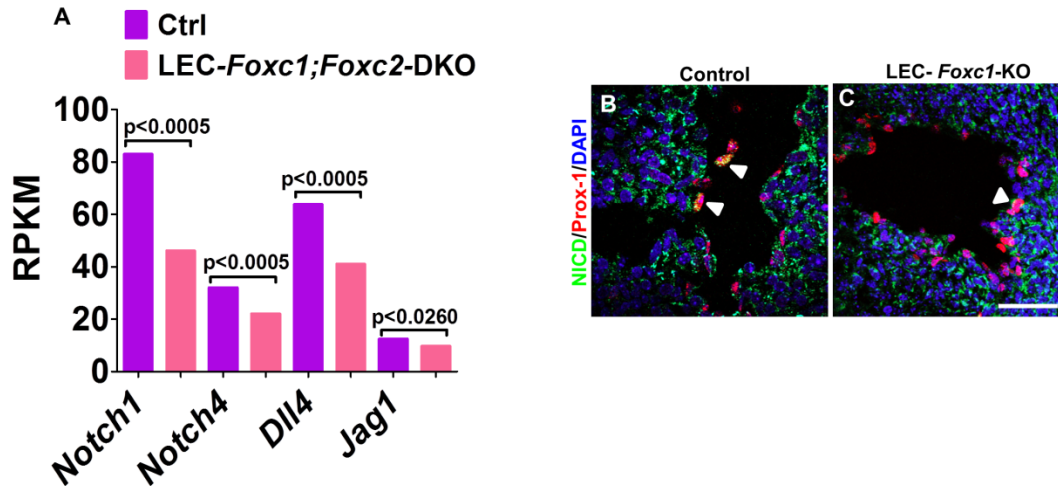
Supplemental Figure 7



Supplemental Figure 7. Lymphatic valve formation in the collecting lymphatic vessels is impaired in *Foxc1* mutants. (A-E) Defective lymphatic valve morphogenesis in LEC-*Foxc1*-KO embryos at E18.5. (A, B) Control valves have reoriented Prox1high cells (arrowheads), while Prox1high cells were not clustered and not reoriented in LEC-*Foxc1*-KO embryos (C, D). Arrows indicate Prox1high valves. (E) Quantification of reoriented Prox1high cells in valve clusters. Values are mean \pm SEM. P-values were obtained by two-tailed Student's t-test. ** $p < 0.01$. (F-K) Whole-mount immunostaining of P7 mesenteric lymphatic vessels for Prox1 and Foxc2 showing mature (v-shaped) and immature (non-v-shaped) valves. Lymphatic valves in EC-*Foxc1*-KO mice were immature compared to the control valves. (H, K) Quantification of the

number of mature and immature valves. P-values were obtained by two-tailed Student's t-test. Data are presented as mean \pm SEM. **p < 0.01. n = 4. Scale bar, 50 μ m.

Supplemental Figure 8



Supplemental Figure 8. Reduced Notch signaling in *Foxc*-mutant LECs. (A) Expression of Notch receptors (*Notch1* and *Notch4*) and ligands (*Dll4* and *Jag1*) was reduced in LECs isolated from LEC-*Foxc1;Foxc2*-DKO embryos. Bar graph showing RPKM (reads per kilo base of coding sequence per million mapped) values from RNA-seq of LEC-*Foxc1;Foxc2*-DKO and control LECs isolated from the dorsal skin at E15.5. (B) Double immunostaining for Prox1 and the Notch1 intracellular domain (NICD) at E12.5. Note that LEC-*Foxc1*-KO embryo had decreased levels of NICD (arrows) in the lymph sacs compared to the control. Scale bar, 50 μ m.